10466 *Inorg. Chem.* **2009**, *48*, 10466–10474
DOI: 10.1021/ic901726b

Inorganic Chemistry
Article

From Classical Adducts to Frustrated Lewis Pairs: Steric Effects in the Interactions of Pyridines and $B(C_6F_5)_3$

Stephen J. Geier,[†] Austin L. Gille,[‡] Thomas M. Gilbert,[‡] and Douglas W. Stephan*,[†]

[†]*Department of Chemistry, University of Toronto, Toronto, Ontario M5S 3H6, Canada, and*
[‡]*Department of Chemistry & Biochemistry, Northern Illinois University, DeKalb, Illinois 60115*

Received August 31, 2009

The pyridine adducts of $B(C_6F_5)_3$, $(4\text{-}tBu)C_5H_4NB(C_6F_5)_3$ **1**, $((2\text{-}Me)C_5H_4N)B(C_6F_5)_3$ **2**, $((2\text{-}Et)C_5H_4N)B(C_6F_5)_3$ **3**, $((2\text{-}Ph)C_5H_4N)B(C_6F_5)_3$ **4**, $((2\text{-}C_5H_4N)C_5H_4N)B(C_6F_5)_3$ **5**, $(C_9H_7N)B(C_6F_5)_3$ **6**, and $((2\text{-}C_5H_4N)NH(2\text{-}C_5H_4N))B(C_6F_5)_3$ **7**, were prepared and characterized. The B−N bond lengths in **2**−**7** reflect the impact of *ortho*-substitution, increasing significantly with sterically larger and electron-withdrawing substituents. In the case of 2-amino-6-picoline, reaction with $B(C_6F_5)_3$ affords the zwitterionic species $(5\text{-}Me)C_5H_3NH(2\text{-}NH)B(C_6F_5)_3$ **8**. In contrast, lutidine/$B(C_6F_5)_3$ yields an equilibrium mixture containing both the free Lewis acid and base and the adduct $(2,6\text{-}Me_2C_5H_3N)B(C_6F_5)_3$ **9**. This equilibrium has a ΔH of −42(1) kJ/mol and ΔS of −131(5) J/mol·K. Addition of H_2 shifts the equilibrium and yields $[2,6\text{-}Me_2C_5H_3NH][HB(C_6F_5)_3]$ **10**. The corresponding reactions of 2,6-diphenylpyridine or 2-*tert*-butylpyridine with $B(C_6F_5)_3$ showed no evidence of adduct formation and upon exposure to H_2 afforded $[(2,6\text{-}Ph_2)C_5H_3NH][HB(C_6F_5)_3]$ **11** and $[(2\text{-}tBu)C_5H_4NH][HB(C_6F_5)_3]$ **12**, respectively. The energetics of adduct formation and the reactions with H_2 are probed computationally. Crystallographic data for compounds **1**−**10** are reported.

Introduction

Recent advances in main group chemistry have provided opportunities for rather unique small molecule activations. Among these, compounds incorporating "frustrated Lewis pairs" which are mixtures of Lewis acids and bases that do not form adducts because of steric constraints have Lewis acidity and basicity which result in unique abilities to activate small molecules including H_2.[1] Similarly, species with element−element multiple bonds[2] and carbenes[3] have garnered attention as a result of their ability to activate H_2. In the case of frustrated Lewis pairs, this reactivity has been extended to allow the metal-free hydrogenation catalysis of imines, aziridines, borane-bound nitriles,[4] enamines, and silylenol-ethers.[5] In addition, frustrated Lewis pairs have been exploited to effect the activation of tetrahydrofuran,[6] catecholborane,[7] olefins,[8] dienes,[9] terminal alkynes,[10] disulfides,[11] CO_2,[12] and N_2O.[13] The initial frustrated Lewis pairs systems reported were based on bulky phosphines in combination with the Lewis acid $B(C_6F_5)_3$.[14] Since then, linked phosphinoboranes[15] pairs of bulky carbenes,[4b,16] and amines[17] with

*To whom correspondence should be addressed. E-mail: dstephan@chem.utoronto.ca.

(1) (a) Welch, G. C.; San Juan, R. R.; Masuda, J. D.; Stephan, D. W. *Science* **2006**, *314*, 1124. (b) Stephan, D. W. *Dalton Trans.* **2009**, 3129. (c) Stephan, D. W. *Org. Biomol. Chem.* **2008**, *6*, 1535.
(2) Spikes, G. H.; Fettinger, J. C.; Power, P. P. *J. Am. Chem. Soc.* **2005**, *127*, 12232.
(3) Frey, G. D.; Lavallo, V.; Donnadieu, B.; Schoeller, W. W.; Bertrand, G. *Science* **2007**, *316*, 439.
(4) (a) Chase, P. A.; Jurca, T.; Stephan, D. W. *Chem. Commun.* **2008**, 1701. (b) Chase, P. A.; Stephan, D. W. *Angew. Chem., Int. Ed.* **2008**, *47*, 7433.
(5) Spies, P.; Schewendemann, S.; Lange, S.; Kehr, G.; Fröhlich, R.; Erker, G. *Angew. Chem., Int. Ed.* **2008**, *47*, 7543.
(6) (a) Welch, G. C.; Cabrera, L.; Chase, P. A.; Hollink, E.; Masuda, J. D.; Wei, P.; Stephan, D. W. *Dalton Trans.* **2007**, 3407. (b) Welch, G. C.; Prieto, R.; Dureen, M. A.; Lough, A. J.; Labeodan, O. A.; Höltrichter-Rössmann, T.; Stephan, D. W., *Dalton Trans.* **2009**, 1559.
(7) Dureen, M., A.; Lough, A.; Gilbert, T. M.; Stephan, D. W. *Chem. Commun.* **2008**, 4303.
(8) McCahill, J. S. J.; Welch, G. C.; Stephan, D. W. *Angew. Chem., Int. Ed.* **2007**, *46*, 4968.
(9) Ullrich, M.; Seto, K. S.-H.; Lough, A. J.; Stephan, D. W. *Chem. Commun.* **2009**, 2335.
(10) Dureen, M. A.; Stephan, D. W. *J. Am. Chem. Soc.* **2009**, *131*, 8396.
(11) Dureen, M. A.; Welch, G. C.; Gilbert, T. M.; Stephan, D. W. *Inorg. Chem.* **2009**, DOI: 10.1021/ic901590s.
(12) Mömming, C. M.; Otten, E.; Kehr, G.; Fröhlich, R.; Grimme, S.; Stephan, D. W.; Erker, G. *Angew. Chem., Int. Ed.* **2009**, *48*, 6643.
(13) Otten, E.; Neu, R. C.; Stephan, D. W., *J. Am. Chem. Soc.* **2009**, *131*, 9918.
(14) Welch, G. C.; Stephan, D. W. *J. Am. Chem. Soc.* **2007**, *129*, 1880.
(15) Geier, S. J.; Gilbert, T. M.; Stephan, D. W. *J. Am. Chem. Soc.* **2008**, *130*, 12632.
(16) (a) Chase, P.; Gille, A. L.; Gilbert, T.; Stephan, D. W. *Dalton Trans.* **2009**, 7179. (b) Holschumacher, D.; Bannenberg, T.; Hrib, C. G.; Jones, P. G.; Tamm, M. *Angew. Chem., Int. Ed.* **2008**, *47*, 7428. (c) Holschumacher, D.; Taouss, C.; Bannenberg, T.; Hrib, C. G.; Daniliuc, C. G.; Jones, P. G.; Tamm, M. *Dalton Trans.* **2009**, 6927.
(17) (a) Sumerin, V.; Schulz, F.; Atsumi, M.; Wang, C.; Nieger, M.; Leskela, M.; Repo, T.; Pyykkö, P.; Rieger, B. *J. Am. Chem. Soc.* **2008**, *130*, 14117. (b) Sumerin, V.; Schulz, F.; Nieger, M.; Leskela, M.; T., R.; Rieger, B. *Angew. Chem., Int. Ed.* **2008**, *47*, 6001.

 Published on Web 10/07/2009

Scheme 1. Main Group Systems That Activate H_2

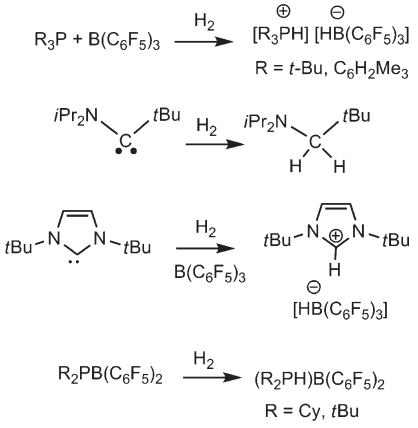

$B(C_6F_5)_3$ and alkyl-linked phosphine-boranes[5,18] have been shown to be effective frustrated Lewis pairs (Scheme 1).

In seeking to explore and broaden the range of bases that can be employed in frustrated Lewis pair chemistry, we were motivated by a 1942 report by Brown et al.[19] In that work, it was reported that 2,6-lutidine was incapable of forming a classical Lewis adduct with BMe_3, as a result of steric conflict of the B-bound methyl groups and the substituents on pyridine. Although Brown and co-workers observed what we now refer to as a frustrated Lewis pairs, they did not explore the resulting reactivity of such systems. In this full account we explore both experimentally and computationally the ability of substituted pyridines and $B(C_6F_5)_3$ to act both as classical Lewis pairs, forming donor−acceptor adducts, and as frustrated Lewis pairs effecting the activation of H_2. A portion of this work has been previously communicated.[20]

Experimental Section

General Considerations. All preparations were done under an atmosphere of dry, O_2-free N_2 employing both Schlenk line techniques and an Innovative Technologies or Vacuum Atmospheres inert atmosphere glovebox. Solvents (pentane, hexanes, toluene, and methylene chloride) were purified employing a Grubbs' type column systems manufactured by Innovative Technology and stored over molecular sieves (4 Å). Molecular sieves (4 Å) were purchased from Aldrich Chemical Co. and dried at 140 °C under vacuum for 24 h prior to use. Deuterated solvents were dried over CaH_2 (CD_2Cl_2, $CDCl_3$) and vacuum distilled prior to use. All common organic reagents were purified by conventional methods unless otherwise noted. All liquid pyridines were stored over 4 Å molecular sieves. ^1H, ^{13}C, ^{11}B, and ^{19}F nuclear magnetic resonance (NMR) spectroscopy spectra were recorded on a Bruker Avance-300 spectrometer at 300 K unless otherwise noted. ^1H and ^{13}C NMR spectra are referenced to $SiMe_4$ using the residual solvent peak impurity of the given solvent. ^{11}B and ^{19}F NMR experiments were referenced to $BF_3(OEt_2)$, and $CFCl_3$, respectively. Chemical shifts are reported in parts per million (ppm) and coupling constants in hertz (Hz) as absolute values. DEPT and 2-D $^1H/^{13}C$ correlation experiments were completed for assignment of the carbon atoms. Combustion analyses were performed in house employing a Perkin-Elmer CHN Analyzer. $B(C_6F_5)_3$ was generously donated by NOVA Chemicals Corporation.

Synthesis of (4-*t*Bu)$C_5H_4NB(C_6F_5)_3$ 1, (2-Me)$C_5H_4NB(C_6F_5)_3$ 2, (2-Et)$C_5H_4NB(C_6F_5)_3$ 3, (2-Ph)$C_5H_4NB(C_6F_5)_3$ 4, (2-$C_5H_4N)C_5H_4NB(C_6F_5)_3$ 5, $C_9H_7NB(C_6F_5)_3$ 6, (2-$C_5H_4N)NH(2$-$C_5H_4N)B(C_6F_5)_3$ 7. These compounds were prepared in a similar fashion and thus only one preparation is detailed. $B(C_6F_5)_3$ (100 mg, 0.20 mmol) was added to a solution of 4-(*t*-Bu)C_5H_4N (26 mg, 0.20 mmol) in 2 mL of toluene. The solution was stirred for 4 h, 2 mL of hexanes was added, and the solution was stored at −35 °C overnight. The solution was decanted from the resulting white precipitate. The precipitate was washed with an additional 2 mL of hexanes and dried in vacuo. Crystals were grown from the hexane wash layer at −35 °C.

1. Yield: 98 mg (78%). ^1H NMR (CD_2Cl_2): 1.40 (s, 9H, CH_3), 7.64 (d, $^3J_{H-H}$ = 7 Hz, 2H), 8.46 (d, $^3J_{H-H}$ = 7 Hz, 2H); ^{19}F NMR (CD_2Cl_2): −132.2 (d, $^3J_{F-F}$ = 19 Hz, 6F, *o*-C_6F_5), −158.2 (t, $^3J_{F-F}$ = 20 Hz, 3F, *p*-C_6F_5), −164.6 (dd, $^3J_{F-F}$ = 19 Hz, $^3J_{F-F}$ = 20 Hz, 6F, *m*-C_6F_5); ^{11}B NMR (CD_2Cl_2): −4.1 (br s); ^{13}C NMR (CD_2Cl_2): 30.0 (*C*H_3), 36.1 (*C*-CH_3), 123.0, 137.4 (dm, $^1J_{C-F}$ = 241 Hz, *C*F), 140.3 (dm, $^1J_{C-F}$ = 260 Hz, *C*F), 146.3, 148.1 (dm, $^1J_{C-F}$ = 248 Hz, *C*F), 168.8. Anal. Calcd for $C_{27}H_{13}BF_{15}N$: C, 50.11%; H, 2.02%; N, 2.16%. Found: C, 50.27%; H, 2.08%; N, 2.16%.

2. Yield: 89%. Crystals were grown from a layered solution of $CDCl_3$/pentane at −35 °C. ^1H NMR ($CDCl_3$): 2.51 (s, 3H, CH_3), 7.43 (m, 2H), 7.99 (td, $^3J_{H-H}$ = 7 Hz, $^4J_{H-H}$ = 2 Hz, 1H), 8.62 (pseudo-q, *J* = 6 Hz, 1H); ^{19}F NMR ($CDCl_3$): −126.3 (m, $^3J_{F-F}$ = 22 Hz, 1F, *o*-C_6F_5), −128.9 (m, 1F, *o*-C_6F_5), −132.4 (d, $^3J_{F-F}$ = 22 Hz, 1F, *o*-C_6F_5), −133.2 (m, 1F, *o*-C_6F_5), −133.4 (m, 1F, *o*-C_6F_5), −137.7 (m, 1F, *o*-C_6F_5), −155.6 (t, $^3J_{F-F}$ = 22 Hz, 1F, *p*-C_6F_5), −156.2 (t, $^3J_{F-F}$ = 22 Hz, 1F, *p*-C_6F_5), −157.7 (t, $^3J_{F-F}$ = 22 Hz, 1F, *p*-C_6F_5), −161.9 (td, $^3J_{F-F}$ = 21 Hz, $^4J_{F-F}$ = 9 Hz, 1F, *m*-C_6F_5), −162.9 (td, $^3J_{F-F}$ = 22 Hz, $^4J_{F-F}$ = 10 Hz, 1F, *m*-C_6F_5), −163.8 (td, $^3J_{F-F}$ = 22 Hz, $^4J_{F-F}$ = 9 Hz, 1F, *m*-C_6F_5), −163.9 (td, $^3J_{F-F}$ = 21 Hz, $^4J_{F-F}$ = 9 Hz, 1F, *m*-C_6F_5), −164.2 (td, $^3J_{F-F}$ = 22 Hz, $^4J_{F-F}$ = 9 Hz, 1F, *m*-C_6F_5), −164.5 (td, $^3J_{F-F}$ = 22 Hz, $^4J_{F-F}$ = 8 Hz, 1F, *m*-C_6F_5); ^{11}B NMR ($CDCl_3$): −3.6; ^{13}C NMR ($CDCl_3$) (partial): 14.3, 122.6, 129.3, 142.3, 147.9, 159.8. Calcd for $C_{24}H_7BF_{15}N$: C, 47.64%; H, 1.17%; N, 2.31%. Found: C, 48.05%; H, 1.38%; N, 2.26%.

3. Yield: 88%. Crystals were grown from the pentane wash layer at room temperature. ^1H NMR (CD_2Cl_2): 0.80 (t, $^3J_{H-H}$ = 8 Hz, 3H, CH_2CH_3), 2.99 (dq, $^2J_{H-H}$ = 23 Hz, $^3J_{H-H}$ = 8 Hz, 1H, CH_2CH_3), 3.05 (dq, $^2J_{H-H}$ = 23 Hz, $^3J_{H-H}$ = 8 Hz, 1H, CH_2CH_3), 7.51 (t, $^3J_{H-H}$ = 7 Hz, 1H), 7.63 (d, $^3J_{H-H}$ = 8 Hz, 1H), 8.15 (td, $^3J_{H-H}$ = 8 Hz, $^4J_{H-H}$ = 1 Hz, 1H), 8.67 (q, *J* = 6 Hz, 1H); ^{19}F NMR (CD_2Cl_2): −126.5 (m, $^3J_{F-F}$ = 22 Hz, 1F, *o*-C_6F_5), −129.6 (m, 1F, *o*-C_6F_5), −132.4 (d, $^3J_{F-F}$ = 22 Hz, 1F, *o*-C_6F_5), −133.7 (m, 1F, *o*-C_6F_5), −134.7 (m, 1F, *o*-C_6F_5), −137.3 (td, $^3J_{F-F}$ = 24 Hz, $^4J_{F-F}$ = 9 Hz, 1F, *o*-C_6F_5), −157.0 (t, $^3J_{F-F}$ = 21 Hz, 1F, *p*-C_6F_5), −157.3 (t, $^3J_{F-F}$ = 20 Hz, 1F, *p*-C_6F_5), −159.2 (t, $^3J_{F-F}$ = 20 Hz, 1F, *p*-C_6F_5), −163.2 (td, $^3J_{F-F}$ = 22 Hz, $^4J_{F-F}$ = 9 Hz, 1F, *m*-C_6F_5), −164.0 (td, $^3J_{F-F}$ = 22 Hz, $^4J_{F-F}$ = 10 Hz, 1F, *m*-C_6F_5), −164.8 (td, $^3J_{F-F}$ = 22 Hz, $^4J_{F-F}$ = 9 Hz, 1F, *m*-C_6F_5), −165.1 (td, $^3J_{F-F}$ = 21 Hz, $^3J_{F-F}$ = 9 Hz, 1F, *m*-C_6F_5), −165.4 (td, $^3J_{F-F}$ = 22 Hz, $^4J_{F-F}$ = 9 Hz, 1F, *m*-C_6F_5), −165.6 (td, $^3J_{F-F}$ = 22 Hz, $^3J_{F-F}$ = 8 Hz, 1F, *m*-C_6F_5); ^{11}B NMR (CD_2Cl_2): −3.6; ^{13}C NMR (CD_2Cl_2) (partial): 13.2, 27.4, 122.6, 127.6, 142.8, 165.5. Calcd for $C_{25}H_9BF_{15}N$: C, 48.50%; H, 1.47%; N, 2.26%. Found: C, 48.25%; H, 1.58%; N, 2.26%.

4. Yield: 85%. Crystals were grown from toluene at room temperature. ^1H NMR ($CDCl_3$): 7.05 (br s, 2H), 7.25 (t, $^3J_{H-H}$ = 8 Hz, 1H), 7.38 (d, $^3J_{H-H}$ = 8 Hz, 1H), 7.40 (br s, 1H), 7.65 (t, $^3J_{H-H}$ = 8 Hz, 1H), 7.85 (br s, 1H), 8.13 (t, $^3J_{H-H}$ = 8 Hz, 1H), 8.93 (s, 1H); ^{19}F NMR ($CDCl_3$): −125.4 (br s, 1F, *o*-C_6F_5), −128.6 (br s, 1F, *o*-C_6F_5), −131.2 (br s, 1F, *o*-C_6F_5), −131.9 (d, $^3J_{F-F}$ = 18 Hz, 1F, *o*-C_6F_5), −133.9 (br s, 2F, *o*-C_6F_5), −155.4 (t, $^3J_{F-F}$ = 20 Hz, 1F, *p*-C_6F_5), −157.7 (br s, 2F, *p*-C_6F_5), −162.0

(18) (a) Spies, P.; Erker, G.; Kehr, G.; Bergander, K.; Fröhlich, R.; Grimme, S.; Stephan, D. W. *Chem. Commun.* **2007**, 5072. (b) Wang, H.; Fröhlich, R.; Kehr, G.; Erker, G. *Chem. Commun.* **2008**, 5966.

(19) Brown, H. C.; Schlesinger, H. I.; Cardon, S. Z. *J. Am. Chem. Soc.* **1942**, *64*, 325.

(20) Geier, S. J.; Stephan, D. W. *J. Am. Chem. Soc.* **2009**, *131*, 3476.

(t, 1F, $^3J_{F-F}$ = 23 Hz, *m*-C_6F_5), −162.9 (t,1F, $^3J_{F-F}$ = 23 Hz, *m*-C_6F_5), −164.5 (br s, 2F, *m*-C_6F_5), −165.1 (br m, 1F, *m*-C_6F_5), −165.6 (br s, 1F, *m*-C_6F_5), ^{11}B NMR ($CDCl_3$): −2.9; ^{13}C NMR ($CDCl_3$) (partial): 124.3, 128.0, 128.5, 129.8, 131.6, 142.3, 148.5. Calcd for $C_{29}H_9BF_{15}N$: C, 52.21%; H, 1.36%; N, 2.10%. Found: C, 51.77%; H, 1.71%; N, 2.32%.

5. Yield: 79%. Crystals were grown from toluene at −35 °C. ^{1}H NMR (CD_2Cl_2): 6.68 (d, $^3J_{H-H}$ = 8 Hz, 1H), 7.16 (ddd, $^3J_{H-H}$ = 8 Hz, $^3J_{H-H}$ = 5 Hz, $^4J_{H-H}$ = 1 Hz, 1H), 7.43−7.48 (ov m, 2H), 7.72 (ddd, $^3J_{H-H}$ = 8 Hz, $^3J_{H-H}$ = 6 Hz, $^4J_{H-H}$ = 2 Hz, 1H), 8.17 (ddd, $^3J_{H-H}$ = 5 Hz, $^4J_{H-H}$ = 2 Hz, $^4J_{H-H}$ = 1 Hz, 1H), 8.23 (td, $^3J_{H-H}$ = 8 Hz, $^4J_{H-H}$ = 2 Hz, 1H), 8.82 (br s, 1H); ^{19}F NMR (CD_2Cl_2): −125.2 (m, 1F, *o*-C_6F_5), −130.9 (m, 1F, *o*-C_6F_5), −131.5 (m, 1F, *o*-C_6F_5), −133.1 (m, 2F, *o*-C_6F_5), −135.6 (d, $^3J_{F-F}$ = 21 Hz, 1F, *o*-C_6F_5), −156.7 (t, $^3J_{F-F}$ = 19 Hz, 1F, *p*-C_6F_5), −158.3 (m, 1F, *p*-C_6F_5), −160.0 (t, $^3J_{F-F}$ = 21 Hz, 1F, *p*-C_6F_5), −160.5 (m, 1F, *m*-C_6F_5), −163.3 (t, $^3J_{F-F}$ = 21 Hz, 1F, *m*-C_6F_5), −163.8 (t, $^3J_{F-F}$ = 21 Hz, 1F, *m*-C_6F_5), −166.0 (t, $^3J_{F-F}$ = 20 Hz, 1F, *m*-C_6F_5), −166.5 (m, 1F, *m*-C_6F_5), −167.6 (m, 1F, *m*-C_6F_5); ^{11}B NMR (CD_2Cl_2): −2.7; ^{13}C NMR ($CDCl_3$) (partial): 123.7, 124.0, 125.0, 130.8, 136.4, 142.8, 148.5, 149.3, 153.6, 158.9. Calcd for $C_{28}H_8BF_{15}N_2$: C, 50.33%; H, 1.21%; N, 4.19%. Found: C, 49.87%; H, 1.44%; N, 4.32%.

6. Yield: 96%. ^{1}H NMR ($CDCl_3$): 7.77 (m, 2H), 7.84 (m, 1H), 8.09 (dd, $^3J_{H-H}$ = 8 Hz, $^4J_{H-H}$ = 2 Hz, 1H), 8.51 (d, $^3J_{H-H}$ = 9 Hz, 1H), 8.72 (d, $^3J_{H-H}$ = 8 Hz, 1H), 9.19 (q, $^3J_{H-H}$ = 5 Hz, 1H); ^{19}F NMR ($CDCl_3$): −126.6 (m, $^3J_{F-F}$ = 27 Hz, 1F, *o*-C_6F_5), −128.8 (br m, 1F, *o*-C_6F_5), −131.9 (br m, 1F, *o*-C_6F_5), −132.9 (m, $^3J_{F-F}$ = 36 Hz, 1F, *o*-C_6F_5), −133.3 (br m, 1F, *o*-C_6F_5), −133.7 (m, 1F, *o*-C_6F_5), −155.1 (tt, $^3J_{F-F}$ = 20 Hz, $^4J_{F-F}$ = 4 Hz, 1F, *p*-C_6F_5), −156.2 (tt, $^3J_{F-F}$ = 20 Hz, $^4J_{F-F}$ = 3 Hz, 1F, *p*-C_6F_5), −157.2 (tt, $^3J_{F-F}$ = 20 Hz, $^4J_{F-F}$ = 3 Hz, 1F, *p*-C_6F_5), −161.2 (td, $^3J_{F-F}$ = 21 Hz, $^4J_{F-F}$ = 8 Hz, 1F, *m*-C_6F_5), −162.3 (td, $^3J_{F-F}$ = 23 Hz, $^4J_{F-F}$ = 10 Hz, 1F, *m*-C_6F_5), −163.2 (td, $^3J_{F-F}$ = 22 Hz, $^4J_{F-F}$ = 8 Hz, 1F, *m*-C_6F_5), −163.7 (td, $^3J_{F-F}$ = 22 Hz, $^4J_{F-F}$ = 9 Hz, 1F, *m*-C_6F_5), −163.8 (m, peaks overlapping, *m*-C_6F_5), −163.9 (m, peaks overlapping, 1F, *m*-C_6F_5); ^{11}B NMR ($CDCl_3$): −3.2; ^{13}C NMR ($CDCl_3$) (partial): 120.2, 122.4, 128.6, 129.6, 130.1, 133.1, 142.6, 145.0, 150.4, $C_{27}H_7BF_{15}N$: C, 50.58%; H, 1.10%; N, 2.18%. Found: C, 50.23%; H, 0.98%; N, 2.35%.

7. Yield: 86%. X-ray quality crystals were grown by slow evaporation from CD_2Cl_2. ^{1}H NMR (CD_2Cl_2): 6.44 (d, $^3J_{H-H}$ = 8 Hz, 1H), 6.96 (dd, $^3J_{H-H}$ = 7 Hz, $^3J_{H-H}$ = 5 Hz, 2H), 7.02 (td, $^3J_{H-H}$ = 7 Hz, $^4J_{H-H}$ = 1 Hz, 1H), 7.55 (td, $^3J_{H-H}$ = 8 Hz, $^4J_{H-H}$ = 2 Hz, 1H), 7.67 (br s, N*H*), 7.91 (ddd, $^3J_{H-H}$ = 9 Hz, $^3J_{H-H}$ = 7 Hz, $^4J_{H-H}$ = 2 Hz, 1H), 8.21 (m, 2H), 8.58 (d, $^3J_{H-H}$ = 9 Hz, 1H); ^{19}F NMR (CD_2Cl_2): −127.0 (m, 1F, *o*-C_6F_5), −128.1 (m, 1F, *o*-C_6F_5), −131.6 (d, $^3J_{F-F}$ = 23 Hz, 1F, *o*-C_6F_5), −133.0 (m, 1F, *o*-C_6F_5); −135.7 (m, 1F, *o*-C_6F_5), −137.1 (m, 1F, *o*-C_6F_5), −157.0 (t, $^3J_{F-F}$ = 20 Hz, 3F, *p*-C_6F_5), −163.0 (td, $^3J_{F-F}$ = 22 Hz, $^4J_{F-F}$ = 8 Hz, 1F, *m*-C_6F_5), −163.9 (tt, $^3J_{F-F}$ = 22 Hz, $^4J_{F-F}$ = 9 Hz, 2F, *m*-C_6F_5), −164.0 (td, $^3J_{F-F}$ = 21 Hz, $^4J_{F-F}$ = 7 Hz, 1F, *m*-C_6F_5), −164.2 (td, $^3J_{F-F}$ = 22 Hz, $^4J_{F-F}$ = 8 Hz, 1F, *m*-C_6F_5); ^{11}B NMR (CD_2Cl_2): −5.1; ^{13}C NMR (CD_2Cl_2) (partial): 139.0, 142.8, 144.1 (m), 148.2, 151.2, 152.4 (m). Anal. Calcd for $C_{28}H_9BF_{15}N_3$: C, 49.23%; H, 1.33%; N, 6.15%. Found: C, 49.59%; H, 1.69%; N, 6.13%.

Synthesis of (5-Me)C_5H_3NH(2-NH)B(C_6F_5)$_3$ 8. 2-Amino-6-picoline (4.5 mg, 0.04 mmol) was added to a solution of B(C_6F_5)$_3$ (20 mg, 0.039 mmol) in 2 mL of CH_2Cl_2. The solution was allowed to stand for 2 h, then all volatiles were removed and the residue was washed with pentane (2 × 2 mL). The resulting white solid was again pumped to dryness. Yield: 23 mg (96%). X-ray quality crystals were grown from a layered solution of $CDCl_3$/pentane at room temperature. ^{1}H NMR ($CDCl_3$): 2.13 (s, 3H, CH_3), 6.07 (br s, 1H, amide N-*H*), 6.23 (dm, $^3J_{H-H}$ = 7 Hz, 1H), 6.55 (br d, $^3J_{H-H}$ = 9 Hz, 1H), 7.38 (dd, $^3J_{H-H}$ = 9 Hz, $^3J_{H-H}$ = 7 Hz), 8.65 (br s, 1H, pyridinium N-*H*); ^{19}F NMR ($CDCl_3$): −133.7 (d, $^3J_{F-F}$ = 20 Hz, 6F, *o*-C_6F_5), −157.0 (t, $^3J_{F-F}$ = 19 Hz, 3F, *p*-C_6F_5), −163.0 (br s, 6F, *m*-C_6F_5); ^{11}B NMR ($CDCl_3$): −11.1; ^{13}C NMR ($CDCl_3$) (partial): 19.3, 109.5, 114.5, 137.0 (dm, $^1J_{C-F}$ = 256 Hz, C*F*), 141.8, 142.3 (dm, $^1J_{C-F}$ = 242 Hz, C*F*), 148.1 (dm, $^1J_{C-F}$ = 240 Hz, C*F*), 155.2. Anal. Calcd for $C_{24}H_8BF_{15}N_2$: C, 46.48%; H, 1.30%; N, 4.52%. Found: C, 46.30%; H, 1.18%; N, 5.02%.

Synthesis of (2,6-$Me_2C_5H_3$N)B(C_6F_5)$_3$ 9. B(C_6F_5)$_3$ (100 mg, 0.20 mmol) was added to 2,6-lutidine (21 mg, 0.20 mmol) in 2 mL of toluene. The solution was allowed to stir for 4 h and 2 mL of pentane was added. The solution was stored at −35 °C. X-ray quality crystals precipitated from solution and were washed with pentane (2 × 2 mL) and again pumped to dryness. Yield: 60 mg (51%). NMR data were acquired at −10 °C. ^{1}H NMR (CD_2Cl_2): 2.58 (s, CH_3), 7.36 (d, 2H, $^3J_{H-H}$ = 8 Hz, *m*-C*H*), 7.89 (t, 1H, $^3J_{H-H}$ = 8 Hz, *p*-C*H*); ^{19}F NMR (CD_2Cl_2): −131.4 (br s, 2F, *o*-C_6F_5), −132.4 (br s, 2F, *o*-C_6F_5), −133.0 (d, 2F, $^3J_{F-F}$ = 18 Hz, *o*-C_6F_5), −157.6 (t, 1F, $^3J_{F-F}$ = 20 Hz, *p*-C_6F_5), −158.7 (t, 2F, $^3J_{F-F}$ = 20 Hz, *p*-C_6F_5), −164.4 (t, 2F, $^3J_{F-F}$ = 21 Hz, *m*-C_6F_5), −165.2 (m, 4F, *m*-C_6F_5); ^{11}B NMR (CD_2Cl_2): −3.9. Anal. Calcd for $C_{31}H_{17}BF_{15}NO_4$: C, 48.50%; H, 1.47%; N, 2.26%. Found: C, 48.70%; H, 1.85%; N, 2.23%.

Synthesis of [2,6-$Me_2C_5H_3$NH][HB(C_6F_5)$_3$] 10, [(2,6-Ph_2)-C_5H_3NH][HB(C_6F_5)$_3$] 11, [(2-*t*Bu)C_5H_4NH][HB(C_6F_5)$_3$] 12. These compounds were prepared in a similar fashion and thus only one preparation is detailed. B(C_6F_5)$_3$ (100 mg, 0.20 mmol) was added to of 2,6-lutidine (21 mg, 0.20 mmol) in 10 mL of toluene. The solution was subjected to 3 freeze−pump−thaw cycles and backfilled with H_2 at 77 K (~4 atm). The solution was allowed to stir overnight at room temperature and then pumped to dryness. The solid was washed with pentane (2 × 2 mL) and again pumped to dryness.

10. Yield: 105 mg (87%). X-ray quality crystals were grown by slow evaporation of a toluene solution. ^{1}H NMR (CD_2Cl_2): 2.61 (s, 6H, CH_3), 3.55 (q, $^1J_{B-H}$ = 88 Hz, B-*H*), 7.53 (d, $^3J_{H-H}$ = 8 Hz, 2H, *m*-C*H*), 8.22 (t, 1H, $^3J_{H-H}$ = 8 Hz, *p*-C*H*), 12.01 (br s, 1H, N-*H*); ^{19}F NMR (CD_2Cl_2): −136.8 (br d, 6F, $^3J_{F-F}$ = 18 Hz, *o*-C_6F_5), −165.8 (t, 3F $^3J_{F-F}$ = 20 Hz, *p*-C_6F_5), −169.3 (br t, 6F, $^3J_{F-F}$ = 20 Hz, *m*-C_6F_5); ^{11}B NMR (CD_2Cl_2): −24.7 (d, $^1J_{B-H}$ = 88 Hz); ^{13}C NMR (CD_2Cl_2) (partial): 19.9, 125.5, 136.7 (dm, $^1J_{C-F}$ = 245 Hz C*F*), 138.4 (dm, $^1J_{C-F}$ = 249 Hz, C*F*), 147.2, 148.2, (dm, $^1J_{C-F}$ = 238 Hz, C*F*), 153.8. Anal. Calcd for $C_{26}H_{11}BF_{15}N$: C, 48.34%; H, 1.78%; N, 2.25%. Found: C, 48.49%; H, 2.06%; N, 2.43%.

11. Yield: 82%. X-ray quality crystals were grown from dichloromethane. ^{1}H NMR (CD_2Cl_2): 3.35 (q, $^1J_{B-H}$ = 92 Hz, B-*H*), 7.57−7.62 (m, 4H), 7.64−7.68 (m, 2H), 7.74−7.77 (m, 4H), 8.05 (d, $^3J_{H-H}$ = 8 Hz, 2H, *m*-C*H*), 8.51 (t, $^3J_{H-H}$ = 8 Hz, 1H, *p*-C*H*), 11.27 (br s, 1H, N-*H*); ^{19}F NMR (CD_2Cl_2): −134.3 (br d, $^3J_{F-F}$ = 21 Hz, 6F, *o*-C_6F_5), −164.8 (t, $^3J_{F-F}$ = 20 Hz, 3F, *p*-C_6F_5), −167.7 (br t, $^3J_{F-F}$ = 20 Hz, 6F, *m*-C_6F_5); ^{11}B NMR (CD_2Cl_2): −24.6 (d, $^1J_{B-H}$ = 92 Hz); ^{13}C NMR (CD_2Cl_2) (partial): 122.6, 126.9, 127.5, 130.2, 132.4. Anal. Calcd for $C_{35}H_{15}BF_{15}N$: C, 56.40%; H, 2.03%; N, 1.88%. Found: C, 56.19%; H, 2.18%; N, 2.09%.

12. Yield: 105 mg (83%). ^{1}H NMR (CD_2Cl_2): 1.51 (s, 9H, C−CH_3), 3.66 (q, $^1J_{B-H}$ = 88 Hz, 1H, B-*H*), 7.80 (t, $^3J_{H-H}$ = 7 Hz, 1H), 7.96 (d, $^3J_{H-H}$ = 8 Hz, 1H), 8.45 (dd, $^3J_{H-H}$ = 8 Hz, $^4J_{H-H}$ = 2 Hz, 1H), 8.48 (d, $^3J_{H-H}$ = 7 Hz, 1H), 12.13 (br s, 1H, N-*H*); ^{19}F NMR (CD_2Cl_2): −134.7 (br d, $^3J_{F-F}$ = 22 Hz, 6F, *o*-C_6F_5), −163.6 (t, $^3J_{F-F}$ = 21 Hz, 3F, *p*-C_6F_5), −167.1 (m, 6F, *m*-C_6F_5); ^{11}B NMR (CD_2Cl_2): −24.7 (d, $^1J_{B-H}$ = 87 Hz); ^{13}C NMR (CD_2Cl_2) (partial): 28.8, 37.1, 125.2, 125.3, 136.8 (dm, $^1J_{C-F}$ = 254 Hz, C*F*), 140.7, 147.7, 148.2 (dm, C*F*, $^1J_{C-F}$ = 240 Hz). Anal. Calcd for $C_{27}H_{15}BF_{15}N$: C, 49.95%; H, 2.33%; N, 2.16%. Found: C, 49.76%; H, 2.22%; N, 2.06%.

X-ray Data Collection and Reduction. Crystals were coated in Paratone-N oil in the glovebox, mounted on a MiTegen

Micromount and placed under an N_2 stream, thus maintaining a dry, O_2-free environment for each crystal. The data were collected on a Bruker Apex II diffractometer. The data were collected at 150(±2) K for all crystals. The frames were integrated with the Bruker SAINT software package using a narrow-frame algorithm. Data were corrected for absorption effects using the empirical multiscan method (SADABS).

Structure Solution and Refinement. Non-hydrogen atomic scattering factors were taken from the literature tabulations.[21] The heavy atom positions were determined using direct methods employing the SHELXTL direct methods routine. The remaining non-hydrogen atoms were located from successive difference Fourier map calculations. The refinements were carried out by using full-matrix least-squares techniques on F, minimizing the function $\omega(F_o - F_c)^2$ where the weight ω is defined as $4F_o^2/2\sigma(F_o^2)$ and F_o and F_c are the observed and calculated structure factor amplitudes, respectively. In the final cycles of each refinement, all non-hydrogen atoms were assigned anisotropic temperature factors in the absence of disorder or insufficient data. In the latter cases atoms were treated isotropically. C−H atom positions were calculated and allowed to ride on the carbon to which they are bonded assuming a C−H bond length of 0.95 Å. H-atom temperature factors were fixed at 1.10 times the isotropic temperature factor of the C-atom to which they are bonded. The H-atom contributions were calculated, but not refined. The locations of the largest peaks in the final difference Fourier map calculation as well as the magnitude of residual electron densities in each case were of no chemical significance. Additional details are provided in Table 1 and in the Supporting Information data.

Computational Methods. Initial optimizations were performed with the GAUSSIAN (G98) suite.[22] $(C_5H_5N)B(C_6F_5)_3$ and $(2\text{-}MeC_5H_4N)B(C_6F_5)_3$ were first optimized without constraints at the HF/3-21G level. Examination of the optimized structures by analytical frequency analyses at this level demonstrated them to be minima (no imaginary frequencies). The structures were reoptimized using a two-layer ONIOM approach (denoted ONIOM(MPW1K),[23] using the MPW1K density functional theory (DFT) model[24] and the 6-31+G(d) basis set for the high levels, and the 3-21G basis set for the low levels.[25] The partitioning of these levels for $B(C_6F_5)_3$ moieties was reported previously; all atoms of the pyridine moieties were placed in the high levels.

As optimization of the structure of **9** at the HF/3-21G level gave a B−N distance of about 3.5 Å, it was optimized instead using the ONIOM(MPW1K) approach and a starting structure with a B−N distance of 1.6 Å. This gave the more reasonable optimized structure given in Table 2 and the Supporting Information. Frequency analysis using the ONIOM model demonstrated the structure to be a minimum. For further confirmation, optimization of the structure using the M06/6-311G(d,p) and M06−2x/6-311G(d,p) DFT[26] approaches as implemented in the GAMESS program[27] gave stationary point structures similar to that from the ONIOM calculation. Single point energies using the ONIOM-(MPW1K) structures and the M06, M06−2x, and MP2[28] models and triple-ζ basis sets (Table 2) were determined using the GAMESS program. Relative energies in the Table were corrected using scaled[29] zero point energies (ZPEs) from the frequency analyses.

For **9**, attempts to optimize "weakly interacting" (B−N distances >2.5 Å) and "transition state" structures (located by scans of the potential energy surface for B−N interaction) using both the HF/3-21G and the ONIOM(MPW1K) approaches were undertaken. While stationary points were located, and frequency analyses characterized them appropriately, their B−N bond lengths and relative energies suggested they were metastable artifact points. The "weakly interacting" complex optimized to structures with B−N distances of 3.4 Å (HF) and >5.6 Å (ONIOM(MPW1K)). No stationary transition state point was located at the HF level, while the ONIOM-(MPW1K)-optimized "transition state" structure exhibited a long B−N distance (2.74 Å) and an energy value essentially equal to that of the sum of the reactants. The M06, M06−2x, and MP2 single point energies determined using this structure were less than the sum of the reactant energies (i.e., gave nonphysical negative barriers). Efforts to optimize the transition states using the M06/6-311G(d,p) and M06−2x/6-311G(d,p) models resulted in structures that optimized toward ones similar to those seen using the ONIOM approach, again with nonphysical barrier energies. It was concluded that the potential energy surface for coordination of 2,6-lutidine to $B(C_6F_5)_3$ is essentially flat until the two are close enough to bond, at which point coordination is barrierless or nearly so. Viewed in reverse, the barrier for dissociation of dimethylpyridine from borane equals the endothermicity of the process, and once this is surmounted, further movement of the moieties from each other is essentially thermoneutral.

Optimizations and single point energy calculations in CH_2Cl_2 solvent employed the PCM solvent continuum[30] approach implemented in GAMESS. Default values for solvent and tesserae parameters were employed. Cartesian coordinates of molecules studied at the ONIOM(MPW1K) or M06−2x/6-311G(d,p) levels are available as Supporting Information.

Results and Discussion

The synthesis of pyridine adducts of $B(C_6F_5)_3$ is facile and well precedented in the literature. Indeed the first report of $(C_5H_5N)B(C_6F_5)_3$ appeared in 1966 by Massey and Park.[31] In a similar and straightforward fashion, combination of 4-*t*-butylpyridine and $B(C_6F_5)_3$ yielded the adduct $(4\text{-}tBu)C_5H_4NB(C_6F_5)_3$ **1**. Compound **1** exhibits a ^{11}B NMR resonance

(21) Cromer, D. T.; Waber, J. T. *Int. Tables X-Ray Crystallogr.* **1974**, *4*, 71.
(22) Frisch, M. J.; Trucks, G. W.; Schlegel, H. B.; Scuseria, G. E.; Robb, M. A.; Cheeseman, J. R.; Zakrzewski, V. G.; Montgomery, J. A., Jr.; Stratmann, R. E.; Burant, J. C.; Dapprich, S.; Millam, J. M.; Daniels, A. D.; Kudin, K. N.; Strain, M. C.; Farkas, O.; Tomasi, J.; Barone, V.; Cossi, M.; Cammi, R.; Mennucci, B.; Pomelli, C.; Adamo, C.; Clifford, S.; Ochterski, J.; Petersson, G. A.; Ayala, P. Y.; Cui, Q.; Morokuma, K.; Malick, A. D.; Rabuck, K. D.; Raghavachari, K.; Foresman, J. B.; Cioslowski, J.; Ortiz, J. V.; Baboul, A. G.; Stefanov, B. B.; Liu, G.; Liashenko, A.; Piskorz, P.; Komaromi, I.; Gomperts, R.; Martin, R. L.; Fox, D. J.; Keith, T.; Al-Laham, M. A.; Peng, C. Y.; Nanayakkara, A.; Challacombe, M.; Gill, P. M. W.; Johnson, B.; Chen, W.; Wong, M. W.; Andres, J. L.; Gonzalez, C.; Head-Gordon, M.; Replogle, E. S.; A., P. J. *Gaussian 98*, Revision A.11.4; Gaussian, Inc.: Pittsburgh, PA, 1998.
(23) (a) Dapprich, S.; Komáromi, I.; Byun, K. S.; Morokuma, K.; Frisch, M. J. *J. Mol. Struct.: THEOCHEM* **1999**, *462*, 1. (b) Svensson, M.; Humbel, S.; Morokuma, K. *J. Chem. Phys.* **1996**, *105*, 3654. (c) Svensson, M.; Humbel, S.; Froese, R. D. J.; Matsubara, T.; Sieber, S.; Morokuma, K. *J. Phys. Chem.* **1996**, *100*, 19357. (d) Matsubara, T.; Sieber, S.; Morokuma, K. *Int. J. Quantum Chem.* **1996**, *60*, 1101. (e) Maseras, F.; Morokuma, K. *J. Comput. Chem.* **1995**, *16*, 1170.
(24) (a) Lynch, B. J.; Truhlar, D. G. *J. Phys. Chem. A* **2001**, *105*, 2936. (b) Adamo, C.; Barone, V. *J. Chem. Phys.* **1998**, *108*, 664.
(25) Gille, A. L.; Gilbert, T. M. *J. Chem. Theory Comput.* **2008**, *3*, 1681.
(26) Zhao, Y.; Truhlar, D. G. *Theor. Chem. Acc.* **2008**, *120*, 215.
(27) (a) Schmidt, M. W.; Baldridge, K. K.; Boatz, J. A.; Elbert, S. T.; Gordon, M. S.; Jensen, J. J.; Koseki, S.; Matsunaga, N.; Nguyen, K. A.; Su, S.; Windus, T. L.; Dupuis, M.; Montgomery, J. A. *J. Comput. Chem.* **1993**, *14*, 1347. (b) Gordon, M. S.; Schmidt, M. W. In *Theory and Applications of Computational Chemistry: The First Forty Years*; Dykstra, C. E., Frenking, G., Kim, K. S., Scuseria, G. E., Eds.; Elsevier: Amsterdam, 2005; p 1167.
(28) Moller, C.; Plesset, M. S. *Phys. Rev.* **1934**, *46*, 618.
(29) (a) Scott, A. P.; Radom, L. *J. Phys. Chem.* **1996**, *100*, 16502. (b) No scaling factor exists for the ONIOM(MPW1K method. However, work of the Truhlar group suggests that all MPW1K methods exhibit scaling factors of ca. 0.95. Therefore we used 0.95 as the scaling factor for the ONIOM(MPW1K) ZPEs. See: ttp://comp.chem.umn.edu/database/freq_scale.htm.
(30) (a) Fedorov, D. G.; Kitaura, K.; Li, H.; Jensen, J. H.; Gordon, M. S. *J. Comput. Chem.* **2006**, *27*, 976. (b) Li, H.; Jensen, J. H. *J. Comput. Chem.* **2004**, *25*, 1449. (c) Tomasi, J.; Mennucci, B.; Cammi, R. *Chem. Rev.* **2005**, *105*, 2999. (d) Cammi, R.; Tomasi, J. *J. Comput. Chem.* **1995**, *16*, 1449.
(31) Massey, A. G.; Park, A. J. *J. Organomet. Chem.* **1966**, *5*, 218.

Table 1. Crystallographic Data[a]

	1	**2**-0.5$CHCl_3$	**3**	**4**-0.5C_7H_8	**5**
formula	$C_{27}H_{13}BF_{15}N$	$C_{24.5}H_{7.5}BCl_{1.5}F_{15}N$	$C_{25}H_9BF_{15}N$	$C_{32.5}H_{13}BF_{15}N$	$C_{28}H_8BF_{15}N_2$
fFormula weight	647.19	664.80	619.14	713.25	668.17
crystal system	monoclinic	monoclinic	triclinic	monoclinic	monoclinic
space group	$P2_1/n$	$P2_1/n$	$P\bar{1}$	$P2_1/n$	$P2_1/c$
a (Å)	11.5466(4)	9.2940(8)	9.7020(9)	9.0823(18)	10.706(2)
b (Å)	13.3174(5)	14.3404(14)	11.5301(11)	15.684(3)	16.332(3)
c (Å)	16.5172(6)	18.4081(18)	12.1581(11)	20.242(4)	14.368(3)
α (deg)	90.00	90.00	105.149(5)	90.00	90.00
β (deg)	92.0820(10)	98.874(4)	94.518(5)	101.05(3)	91.27(3)
γ (deg)	90.00	90.00	113.003(4)	90.00	90.00
V (Å^3)	2538.18(16)	2424.1(4)	1183.10(19)	2830.0(10)	2511.6(8)
Z	4	4	2	4	4
d(calc) g cm^{-1}	1.694	1.822	1.738	1.674	1.767
μ, cm^{-1}	0.176	0.347	0.185	0.167	0.182
data: total (indep)	6669	5542	7401	6440	4389
data $F_o^2 > 3\sigma(F_o^2)$	4924	3159	5857	4163	2499
variables	397	401	379	466	415
R[b]	0.0392	0.0528	0.0427	0.0522	0.0504
R_w[c]	0.0938	0.1270	0.1238	0.1506	0.1409
goodness of fit	1.020	1.007	1.093	1.045	1.006
	6	**7**	**8**	**9**	**10**
formula	$C_{27}H_7BF_{15}N$	$C_{28}H_9BF_{15}N_3$	$C_{24}H_8BF_{15}N_2$	$C_{25}H_9BF_{15}N$	$C_{25}H_{11}BF_{15}N$
formula weight	641.15	683.19	620.13	619.14	621.16
crystal system	Triclinic	Triclinic	Triclinic	Monoclinic	Monoclinic
space group	$P\bar{1}$	$P\bar{1}$	$P\bar{1}$	$P2_1/n$	$P2_1/c$
a (Å)	9.9848(9)	9.6501(10)	9.8535(13)	12.8108(4)	17.8525(12)
b (Å)	10.9162(10)	9.7264(8)	11.1355(16)	13.4663(4)	9.8407(7)
c (Å)	11.6538(11)	14.9925(11)	11.5291(16)	13.3937(4)	15.2683(10)
α (deg)	107.046(5)	107.830(3)	74.467(8)	90.00	90.00
β (deg)	94.178(5)	102.077(4)	73.964(7)	100.156(2)	115.010(3)
γ (deg)	101.061(5)	98.166(3)	80.673(7)	90.00	90.00
V (Å^3)	1180.52(19)	1277.46(19)	1166.1(3)	2274.40(12)	2430.8(3)
Z	2	2	2	4	4
d(calc) g cm^{-1}	1.804	1.776	1.697	1.808	1.697
μ, cm^{-1}	0.189	0.182	0.189	0.192	0.180
data: total (indep)	5413	6580	12524	7942	8206
data $F_o^2 > 3\sigma(F_o^2)$	4093	4246	7552	6118	4499
variables	397	424	388	379	383
R[b]	0.0549	0.0427	0.0416	0.0494	0.0516
R_w[c]	0.0903	0.1017	0.1383	0.1475	0.1680
Goodness of Fit	1.017	1.020	1.007	1.055	1.005

[a] This data were collected at 150 K with Mo Kα radiation (λ = 0.71069 Å). [b] $R = \sum||F_o| - |F_c||/\sum|F_o|$. [c] $R_w = (\sum w(F_o^2 - F_c^2)^2/\sum w(F_o)^2])^{1/2}$.

Table 2. Computational Energies (kJ/mol) for Models of $B(C_6F_5)_3$/Pyridine Interactions

	B−N[a]	ONIOM[b]	M06[c]	M06−2x[c]	MP2[d]
$(C_5H_5N)B(C_6F_5)_3$	1.616 (1.628)	−120	−108	−138	−177
(2-MeC_5H_4N)-$B(C_6F_5)_3$	1.634 (1.639)	−102	−100	−133	−166
(2,5-$Me_2C_5H_4N$)-$B(C_6F_5)_3$	1.653 (1.661)	−61	−69	−103	−153

[a] Calcd (exptl) B−N bond distance. [b] Basis set: ONIOM(MPW1K). [c] Basis set: 6-311G(d,p), [d] Basis set: 6-311++G(d,p).

at −4.1 ppm consistent with quaternization of B, while the ^{1}H and ^{13}C NMR data were also consistent with the adduct formulation. The ^{19}F NMR spectrum of **1** shows resonances at −132.2, −158.2, and −164.6 ppm consistent with 3-fold molecular symmetry in solution. Crystallographic data for **1** (Figure 1) showed a B−N distance of 1.618(2) Å. This compares to the B−N distance of 1.628(2) Å[32] in $(C_5H_5N)B(C_6F_5)_3$,[33] consistent with the notion that electron-donating substitution remote to N results in a shortened B−N bond relative to that of the pyridine adduct.

A series of adducts with substitution in the *ortho*-position were examined. The species ((2-Me)C_5H_4N)$B(C_6F_5)_3$ **2**, ((2-Et)C_5H_4N)$B(C_6F_5)_3$ **3**, ((2-Ph)C_5H_4N)$B(C_6F_5)_3$ **4**, ((2-C_5H_4N)C_5H_4N)$B(C_6F_5)_3$ **5**, $(C_9H_7N)B(C_6F_5)_3$ **6**, ((2-C_5H_4N)NH-(2-C_5H_4N))$B(C_6F_5)_3$ **7** were readily achieved (Scheme 2). NMR data for **2**−**7** showed the expected ^{11}B resonances in the vicinity of −3 to −5 ppm. In contrast to **1**, species **2**−**7** exhibit ^{19}F NMR spectra that are composed of 15 signals reflecting the molecular dissymmetry of these products and restricted rotation about the B−N bonds (Figure 2). Crystallographic data for **2**−**7** (Figure 3−5) reveals the structural impact of *ortho*-substitution. The B−N distances in **2**−**7** were found to be 1.639(4) Å, 1.638(2) Å, 1.654(7) Å, 1.649(5) Å, 1.641(2) Å, and 1.629(2) Å, respectively. The lengthening of the B−N bonds in **2**−**7** reflects the steric impact of *ortho*-substitution. The B−N bond lengths for **2** and **3** are similar and yet significantly shorter than those

(32) (a) Piers, W. E. *Adv. Organomet. Chem.* **2005**, *52*, 1. (b) Focante, F.; Mercandelli, P.; Sironi, A.; Resconi, L. *Coord. Chem. Rev.* **2006**, *250*, 170.
(33) Lesley, M. J. G.; Woodward, A.; Taylor, N. J.; Marder, T. B.; Cazenobe, I.; Ledoux, I.; Zyss, J.; Thornton, A.; Bruce, D. W.; Kakkar, A. K. *Chem. Mater.* **1998**, *10*, 1355.

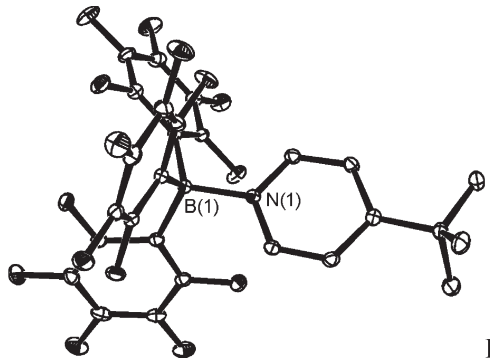

Figure 1. ORTEP drawing of **1**, 50% thermal ellipsoids are shown, hydrogen atoms are omitted for clarity. Selected bond distances (Å) and angles (deg).

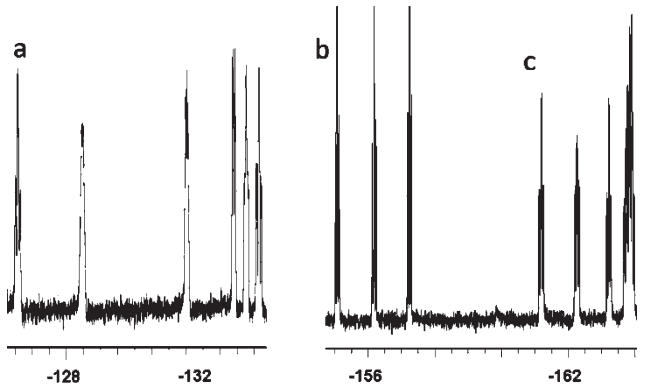

Figure 2. ^{19}F NMR spectrum of **6** (a: *ortho*-C_6F_5, b: *para*-C_6F_5, c: *meta*-C_6F_5).

Scheme 2. Synthesis of **1**−**7**

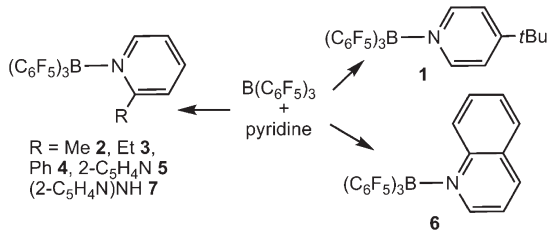

in **4** and **5** consistent with the larger steric demands and increased electron-withdrawing abilities of the phenyl and pyridyl substituents. Similarly for **6**, the increased steric bulk of and reduced basicity of quinoline results in a B−N distance significantly longer than that seen in $(C_5H_5N)B(C_6F_5)_3$.[33]

Introduction of a second *ortho*-substituent on pyridine provides interesting and contrasting reactivity. The reaction of $B(C_6F_5)_3$ with 2-amino-6-picoline proceeds to give the product **8**. Quaternization of B is evident from the ^{11}B NMR signal as −11.1 ppm, suggesting anionic character at B. The corresponding ^{19}F NMR spectrum shows signals at −133.7, −157.0, and −163.0 ppm. The absence of a more complex spectrum suggests that B does not coordinate to the pyridyl nitrogen. ^{1}H NMR resonances at 6.07 and 8.65 ppm suggest the presence of amide and pyridinium protons. Crystallographic data for **8** revealed the amine N of 2-amino-6-picoline coordinates to B and a proton is transferred to the pyridyl N affording a zwitterionic species (5-Me)C_5H_3NH(2-NH)B-$(C_6F_5)_3$ **8** (Figure 6, Scheme 3). As a result, the B−N distance

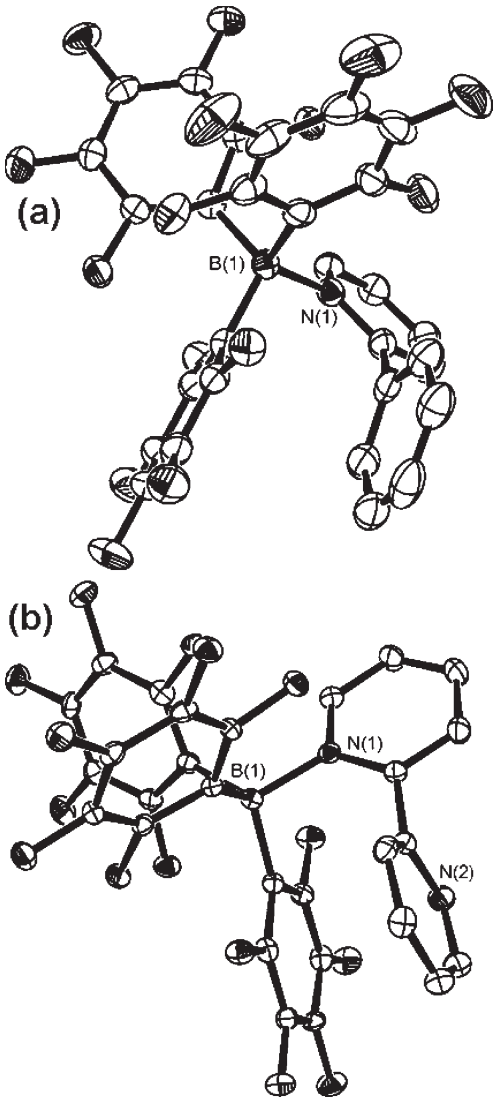

Figure 3. ORTEP drawings of (a) **2**, (b) **3**, 50% thermal ellipsoids are shown, hydrogen atoms are omitted for clarity. Selected bond distances (Å) and angles (deg).

of 1.5602(12) Å is substantially shorter than previously characterized amine-$B(C_6F_5)_3$ adducts[32,34] and significantly longer than that seen in the anion $[(C_6H_5NH)B(C_6F_5)_3]^-$ (1.532(8) Å),[4b] reflecting the electron withdrawing nature of the pyridinium fragment in **8**. This bond length in **8** is comparable to B−N distances of 1.552 Å and 1.576 Å, seen in the salts [(12-crown-4)Li][$NH_2B(C_6F_5)_3$][35] and [(Et_2O)Li]-[pyrrolyl $B(C_6F_5)_3$],[36] respectively. This B−N bond length in **8** is also significantly shorter than that reported for the adduct (4-$Me_2NC_5H_4N$)$B(C_6F_5)_3$ (1.602(6) Å) where B binding occurs to the pyridyl N.[33] The N(1)−C(19) bond length is 1.3240(13) Å consistent with the electron-withdrawing nature of pyridinium substituent on the amido-boron linkage. It is interesting to note that although the pyridyl N of 2-amino-6-picoline is more basic than the amine substituent, the amine is

(34) Mountford, A. J.; Lancaster, S. J.; Coles, S. J.; Horton, P. N.; Hughes, D. L.; Hursthouse, M. B.; Light, M. E. *Inorg. Chem.* **2005**, *44*, 5921.
(35) Mountford, A. J.; Clegg, W.; Coles, S. J.; Harrington, R. W.; Horton, P. N.; Humphrey, S. M.; Hursthouse, M. B.; Wright, J. A.; Lancaster, S. J. *Chem.—Eur. J.* **2007**, *13*, 4535.
(36) Kehr, G.; Roesmann, R.; Frohlich, R.; Holst, C.; Erker, G. *Eur. J. Inorg. Chem.* **2001**, 535.

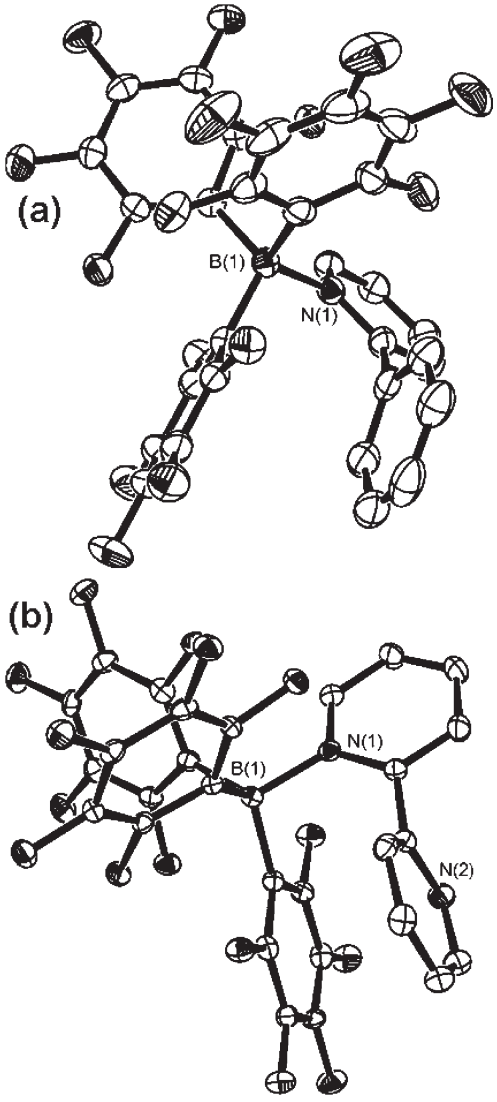

Figure 4. ORTEP drawings of (a) **4**, (b) **5**, 50% thermal ellipsoids are shown, hydrogen atoms are omitted for clarity. Selected bond distances (Å) and angles (deg).

more accessible for coordination to B. Thus, the formation of the zwitterion **8** is a ramification of steric congestion.

Given the departure from conventional reactivity affording **8** the reaction of the disubstituted pyridine 2,6-lutidine and $B(C_6F_5)_3$ was examined. Monitoring the reaction by ^1H and ^{19}F NMR spectra revealed only broad spectral lines, suggesting the existence of equilibrium between free lutidine/$B(C_6F_5)_3$ mixture and the adduct $(2,6\text{-}Me_2C_5H_3N)B(C_6F_5)_3$ **9** (Scheme 4). Variable temperature NMR spectra showed eight ^{19}F NMR resonances at −10 °C consistent with inequivalent C_6F_5-ring environments. This, together with a ^{11}B NMR signal at −3.9 ppm were consistent with the formation of **9**. X-ray crystallographic analysis confirmed the formulation of **9** (Figure 7). The B−N bond length in **9** of 1.661(2) Å is exceptionally longer in comparison to adducts **1**−**7**, presumably a result of the dramatic steric demands limiting the approach of N to B.

The activation parameters associated with the equilibrium process were determined by analysis of the NMR data. This revealed ΔH of −42(1) kJ/mol and ΔS of −131(5) J/mol K. This equilibrium suggests that access to a mixture of free

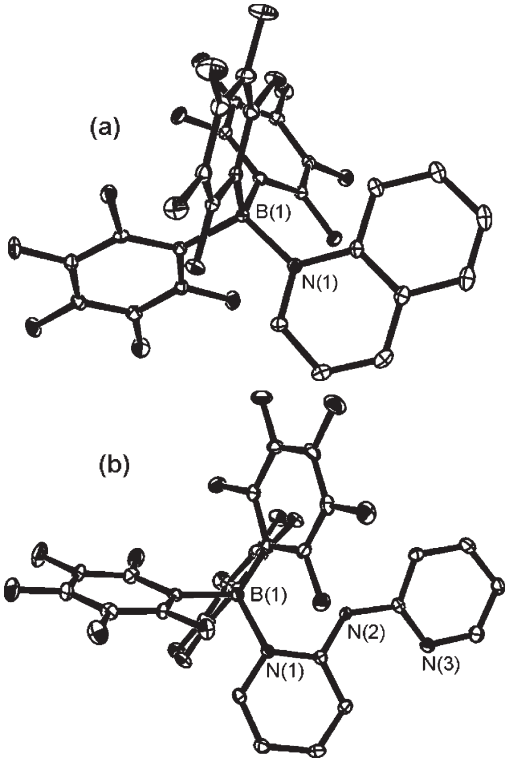

Figure 5. ORTEP drawing of (a) **6**, (b) **7**, 50% thermal ellipsoids are shown, hydrogen atoms are omitted for clarity. Selected bond distances (Å) and angles (deg).

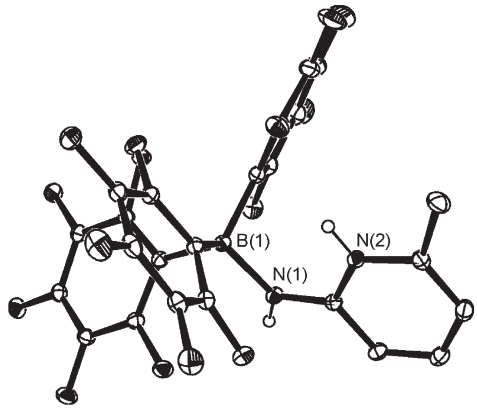

Figure 6. ORTEP drawing of **8**, 50% thermal ellipsoids are shown, hydrogen atoms except for the NH are omitted for clarity. Selected bond distances (Å) and angles (deg).

Scheme 3. Synthesis of **8**

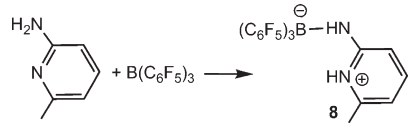

Lewis acid and base could be exploited for frustrated Lewis pair reactivity. Thus, H_2 (1 atm, 2 h) was added to the mixture at 25 °C. This afforded a new product **10** in 87% yield. ^1H NMR data showed resonances at 12.01 and 3.55 ppm, attributable to NH and BH units respectively. These data, together with the ^{19}F and ^{11}B NMR resonances were consistent with the formulation of **10** as $[2,6\text{-}Me_2C_5H_3NH][HB(C_6F_5)_3]$ (Scheme 4). This was confirmed by X-ray diffraction

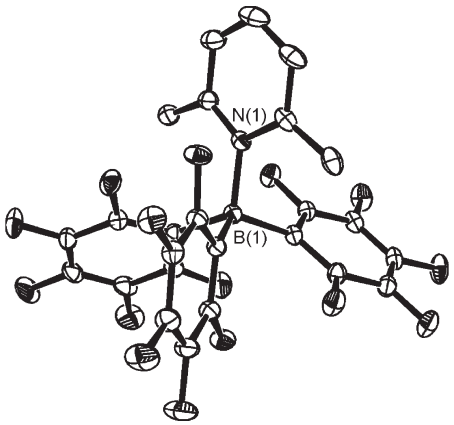

Figure 7. ORTEP drawing of **9**, 50% thermal ellipsoids are shown, hydrogen atoms are omitted for clarity. Selected bond distances (Å) and angles (deg).

Scheme 4. Reactions of Substituted-Pyridines with H_2

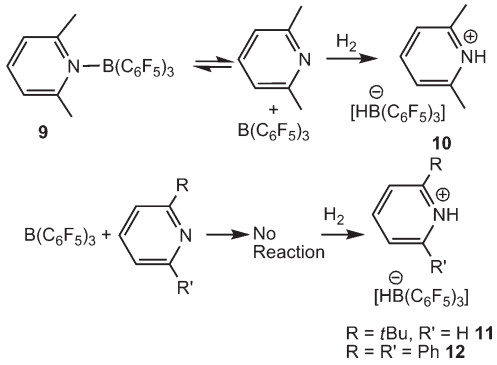

(Figure 8). The metric parameters of this salt have been previously discussed.[20]

Monitoring reactions mixtures of 2,6-diphenylpyridine with $B(C_6F_5)_3$ showed no evidence of reaction by multinuclear NMR spectroscopy even at low temperature. Thus, the increased steric demands of Ph versus Me preclude the classic Lewis donor−acceptor interaction completely. The resulting frustrated Lewis pair reacts upon exposure to H_2 affording the salt $[(2,6\text{-}Ph_2)C_5H_3NH][HB(C_6F_5)_3]$ **11** in 82% yield (Scheme 4).

The above systems suggest that disubstituted pyridines are sufficiently bulky to behave as frustrated Lewis pairs, while monosubstituted pyridines form classic adducts. However, 2-*tert*-butylpyridine, shows no evidence of adduct formation with $B(C_6F_5)_3$ at temperatures as low as −60 °C. This mixture of unquenched Lewis acid and base reacts with 1 atm H_2 in 2 h, affording the quantitative formation of the pyridinium borate salt $[(2\text{-}t\text{Bu})C_5H_4NH][HB(C_6F_5)_3]$ **12** (Scheme 4). NMR data showed the characteristic pyridinium N−H and B−H signals in the ^{1}H NMR spectrum, a broad singlet at 12.13 ppm, and a broad 1:1:1:1 quartet at 3.66 ppm, respectively, as well as the expected ^{11}B and ^{19}F resonances.

It is also interesting to note that generation of a frustrated Lewis pair is not a sufficient condition to effect the heterolytic activation of H_2. For example, the adducts of 2,2′-bipyridine and 2,2′-dipyridylamine, **6** and **7**, respectively, failed to react with a second equivalent of $B(C_6F_5)_3$, presumably a result of a combination of electronic and steric effects. While formally the resulting combinations of these adducts with an unquenched donor and $B(C_6F_5)_3$ are frustrated Lewis pairs, these mixtures did not react with H_2. This stands in contrast to ferrocenyldiphosphines where reaction at one P center provides the steric hindrance affording frustrated Lewis pair activation of H_2 at the other P center.[37] The present result is consistent with the diminished basicity at the free nitrogen resulting from the electron withdrawing effect of the pendant pyridyl-borane adduct. This supports the notion that there is a threshold of cumulative Lewis acidity and basicity required for a frustrated Lewis pair to effect heterolytic H_2 cleavage.[14]

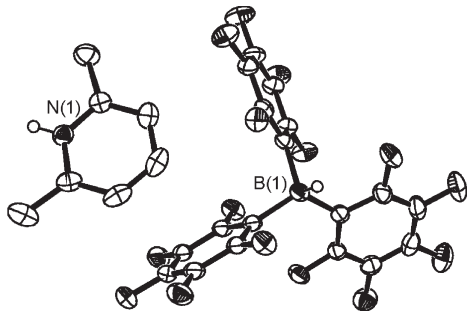

Figure 8. ORTEP drawing of **10**, 50% thermal ellipsoids are shown, hydrogen atoms except for the NH and BH are omitted for clarity. Selected bond distances (Å) and angles (deg).

Computational Studies. To assess the nature of the equilibrium between 2,6-lutidine with $B(C_6F_5)_3$, and to understand the kinetic and thermodynamic differences between this frustrated Lewis pair and the less-substituted analogues, the reactions between $B(C_6F_5)_3$ and pyridine, 2-methylpyridine, and 2,6-lutidine were examined computationally (Table 2). The optimized structures exhibit B−N distances in fine agreement with the experimental values. This is somewhat misleading, given that in general one expects "gas phase" computational distances for dative B−N bonds to be longer than those observed in solid state crystallography studies.[38] The B−N distance increases regularly with the number of methyl groups on the pyridine moiety. Given that complex **9** exists in equilibrium with the frustrated Lewis pair, the predicted B−N distance of 1.65 Å might represent a lower limit for that parameter for reactive frustrated Lewis pairs.

Different models give rather different energy predictions for these complexes. Notably, the predicted exothermicities for formation of **9** are invariably larger than that observed experimentally, substantially so for the MP2 model. Nonetheless, these computational and experimental data illustrate the following: the coordination energy decreases non-linearly as the steric bulk of the pyridine increases, wherein the effect of a single methyl substitution on pyridine is small, while the effect of a second methyl substitution is substantial. The "tipping point" where the energy is sufficiently small to allow equilibrium formation of a frustrated Lewis pair lies in the range 60−100 kJ mol^{-1}. This sets an upper limit on coordination energy that is consistent with that calculated for the very reactive FLP $(F_5C_6)_3B/P\text{t-}Bu_3$ (80 kJ mol^{-1}).[25]

(37) Ramos, A.; Lough, A. J.; Stephan, D. W. *Chem. Commun.* **2009**, 1118.

(38) (a) Phillips, J. A.; Halfen, J. A.; Wrass, J. P.; Knutson, C. C.; Cramer, C. J. *Inorg. Chem.* **2006**, *45*, 722. (b) Dillen, J.; Verhoeven, P. *J. Phys. Chem. A* **2003**, *107*, 2570. (c) Giesen, D. J.; Phillips, J. A. *J. Phys. Chem. A* **2003**, *107*, 4009.

Coordination energies above this range lead to formation of stable Lewis acid−base complexes.

The poor agreement between predicted and experimental coordination energies prompted an examination of solvation effects. Encapsulating the reaction components in CH_2Cl_2 solvent modeled as a polar continuum (PCM model) had little effect on the predicted energy, in keeping with the modest dielectric constant of CH_2Cl_2. This also held when an explicit CH_2Cl_2 molecule was included in the PCM solvent cavity; in particular, binding of Cl lone pairs to the Lewis acidic boron in free $B(C_6F_5)_3$ proved minimal. The B−Cl distance in $(F_5C_6)_3B\cdot Cl_2CH_2$ optimized to 3.12 Å (i.e., the distance expected on the basis of van der Waals radii), while the energy stabilization of this "complex" versus the free molecules was less than 5 kJ mol^{-1}. Apparently the models used here inherently overestimate the coordination energy of **9**; future work will address this problem.

Experimentally, complex **9** reacts with H_2 to form the corresponding pyridinium hydroborate, **10**. The models confirm that this reaction must take place with the frustrated Lewis pair form of the equilibrium system, rather than with the coordinated complex. Calculations for the hydrogenation find that reaction between "free" $B(C_6F_5)_3$ and 2,6-lutidine and H_2 is exothermic by 55−63 kJ mol^{-1}, depending on the model. These compare well with several reported calculations involving dissociation of H_2 from BN systems, although they are on the low side.[39] However, computationally, the reaction between complex **9** and H_2 is *endothermic* by 11−37 kJ mol^{-1}, indicating that the B−N bond in **9** must be broken, or at least substantially weakened through stretching, before hydrogenation.

In summary, systematic variation of the steric bulk of substituents on pyridine prompts elongation of the resulting B−N bonds in classical Lewis acid adducts. Increasing the steric conflict further, as in the case of 2,6-lutidine, 2,6-diphenylpyridine and 2-*tert*-butylpyridine prompts formation of frustrated Lewis pairs, capable of heterolytic activation of H_2. Only 2,6-lutidine was observed to form both a classical Lewis adduct and a frustrated Lewis pair. We continue to explore the scope of reactivity of frustrated Lewis pairs and their applications to hydrogen storage and catalysis.

Acknowledgment. The authors thank NSERC of Canada for financial support. D.W.S. is grateful for the award of a Canada Research Chair and a Killam Research Fellowship. S.J.G. is grateful for an NSERC postgraduate scholarship.

Supporting Information Available: Crystallographic data in CIF format. Ordering information is given on any current masthead page. CIF data is available online. This material is available free of charge via the Internet at http://pubs.acs.org.

(39) (a) Matus, M. H.; Anderson, K. D.; Camaloni, D. M.; Autrey, S. T.; Dixon, D. A. *J. Phys. Chem. A* **2007**, *111*, 4411. (b) Nirmala, V.; Kolandaivel, P. *J. Mol. Struc.: THEOCHEM* **2006**, *758*, 9.